Int. J. Heat Mass Transfer. Vol. 13, pp. 1857–1872. Pergamon Press 1970. Printed in Great Britain

NATURAL CONVECTION HEAT TRANSFER BETWEEN CONCENTRIC SPHERES

J. A. SCANLAN, E. H. BISHOP and R. E. POWE
Montana State University, Bozeman, Montana, U.S.A.

(*Received* 31 *December* 1969 *and in revised form* 10 *March* 1970)

Abstract—An experimental investigation is described concerning natural convection between two isothermal concentric spheres of various diameter ratios ranging from 1·09 to 2·81. The convecting fluids used were water and two silicone oils yielding Prandtl numbers in the range of 4·7–4148 and Rayleigh numbers, based on gap width, in the range of $1{\cdot}3 \times 10^3$–$5{\cdot}8 \times 10^8$. Measured temperature profiles are analyzed in detail with reference to five typical characteristics of the profile shapes. All features of the profiles are explained in terms of postulated convective flow patterns which represent extensions of work previously reported for air under similar conditions. A k_{eff}/k vs. Rayleigh number heat transfer correlation is presented for each of the three fluids individually, and an overall expression based solely on a modified Rayleigh number is presented which correlates all three liquids as well as air. The correlations fit the data with an average deviation of less than 16 per cent.

NOMENCLATURE

$a, b, c, C,$	empirical constants;
$g,$	local gravitational acceleration;
$Gr,$	Grashof number, $g\beta\delta^3(\Delta T)/\nu^2$ (δ may be L, r_i or r_0);
$k,$	thermal conductivity;
$k_{eff},$	effective thermal conductivity defined by equation (1);
$L,$	gap width, $r_0 - r_i$;
$Nu,$	Nusselt number, $qL/4\pi k(\Delta T)r_i^2$;
$Pr,$	Prandtl number, ν/α;
$q,$	natural convection heat-transfer rate;
$r,$	radial coordinate;
$r_{av},$	average radius, $(r_i + r_0)/2$;
$Ra,$	Rayleigh number, $g\beta\delta^3(\Delta T)/(\nu\alpha)$ (δ may be L, r_i or r_0);
$Ra^*,$	modified Rayleigh number $g\beta L^4(\Delta T)/\nu\alpha r_i$);
$T,$	temperature;
$T_m,$	volume weighted mean temperature defined by equation (2);
$\alpha,$	thermal diffusivity;
$\beta,$	thermal expansion coefficient;
$\Delta T,$	temperature difference, $T_i - T_0$;
$\phi,$	angular coordinate measured from upward vertical axis;
$\nu,$	kinematic viscosity.

Subscripts

$i,$	refers to inner sphere;
$o,$	refers to outer sphere;
$L,$	refers to gap width.

1. INTRODUCTION

A CONSIDERABLE amount of work has previously been performed on natural convective heat transfer from a body to an infinite atmosphere, but only limited information is available concerning heat transfer by natural convection from a body to its finite enclosure. This particular heat transfer and fluid mechanics problem is becoming increasingly important in such areas as nuclear design, aircraft cabin design and electronic instrumentation packaging. As a logical first step in the investigation of this problem, several relatively simple geometries, including infinite parallel plates, concentric cylinders and concentric spheres, have been studied both experimentally and analytically.

In the previous investigations for the plate and cylinder geometries, a variety of fluids have been utilized, thus yielding a wide Prandtl number range. Natural convection between concentric spheres, however, has been investigated only for a single Prandtl number, that of air. Utilizing air as the working fluid, Bishop *et al.* [1–3] present experimental data for the heat transfer, temperature profiles, and flow patterns obtained for diameter ratios ranging from 1·19 to 3·14 and Grashof numbers based on gap-thickness ranging from 2×10^4 to $3{\cdot}6 \times 10^6$. Except for the smallest gap–radius ratio ($L/r_i = 0{\cdot}25$) considered, they found the measured temperature distributions to be relatively independent of the temperature difference between the spheres. Their heat-transfer results, for all values of L/r_i, were well represented by an empirical equation giving k_{eff}/k as a function only of the Grashof number based on gap width. In addition to this experimental investigation, an analytical solution for natural convection between concentric spheres at low Rayleigh numbers has been presented by Mack and Hardee [4]. This solution consists of expansions of the temperature and stream function in power series of the Rayleigh number and the evaluation of the first three terms in each of these series. Results of this solution are presented, however, only for a Prandtl number approximately equal to that of air.

The purpose of the current investigation is to greatly extend the range of Prandtl numbers for which heat-transfer data are available for the spherical geometry. An experimental study of the natural convection of fluids contained between a heated inner sphere and a cooled outer sphere is discussed for relative gap widths ranging from 0·09 to 1·81, and temperature profiles and heat-transfer data are presented. The spheres were mounted concentrically, and each was maintained at a constant and uniform temperature. Water and silicone oils were utilized as the fluid in the gap to yield Prandtl numbers ranging from 4·7 to 4148 and Rayleigh numbers, based on gap width, ranging from $1{\cdot}3 \times 10^3$ to $5{\cdot}8 \times 10^8$ were obtained. The results of the current investigation are combined with those of the previous investigation utilizing air to yield detailed descriptions of the temperature profiles and an empirical correlation equation for the heat-transfer data for a very wide range of Prandtl and Rayleigh numbers.

2. HEAT-TRANSFER APPARATUS AND PROCEDURE

The heat-transfer apparatus, shown in Fig. 1, consisted of two concentric spheres enclosed in a water jacket. Values of L/r_i of 0·09, 0·40, 0·79, 1·18 and 1·81 were obtained by utilizing inner spheres of 22·8, 17·8, 13·9, 11·4 and 8·88 cm dia. in conjunction with a single outer sphere of 24·9 cm i.d. The inner spheres were of 0·159 cm thick copper and the outer sphere was of 0·318 cm thick stainless steel.

The inner spheres were supported in the outer sphere by a 1·27 cm dia. stainless steel stem which was insulated on its lateral surface. A uniform inner-sphere surface temperature was achieved by condensing Freon-11 vapor on the inner surface of the sphere. The saturation conditions were varied by changing the power input to electrical disk heaters located within the inner sphere below the Freon liquid level. The surface temperature of the inner sphere was measured by thermocouples located at 90° intervals around the horizontal equator of the sphere. A small stainless steel tube extended through the support stem for pressure measurements within the inner sphere and for venting during Freon charging. Figure 2 is a photograph of the interior of an inner sphere which shows the arrangement of the heaters, thermocouples, and the pressure tube.

The outer sphere consisted of two hemispheres joined by an external flange and sealed with an Ö-ring to facilitate disassembly for changing the inner sphere. Thermocouple probe guides were attached to the outer surface of the sphere. The outer sphere was supported within the water jacket by a stainless steel spacer which

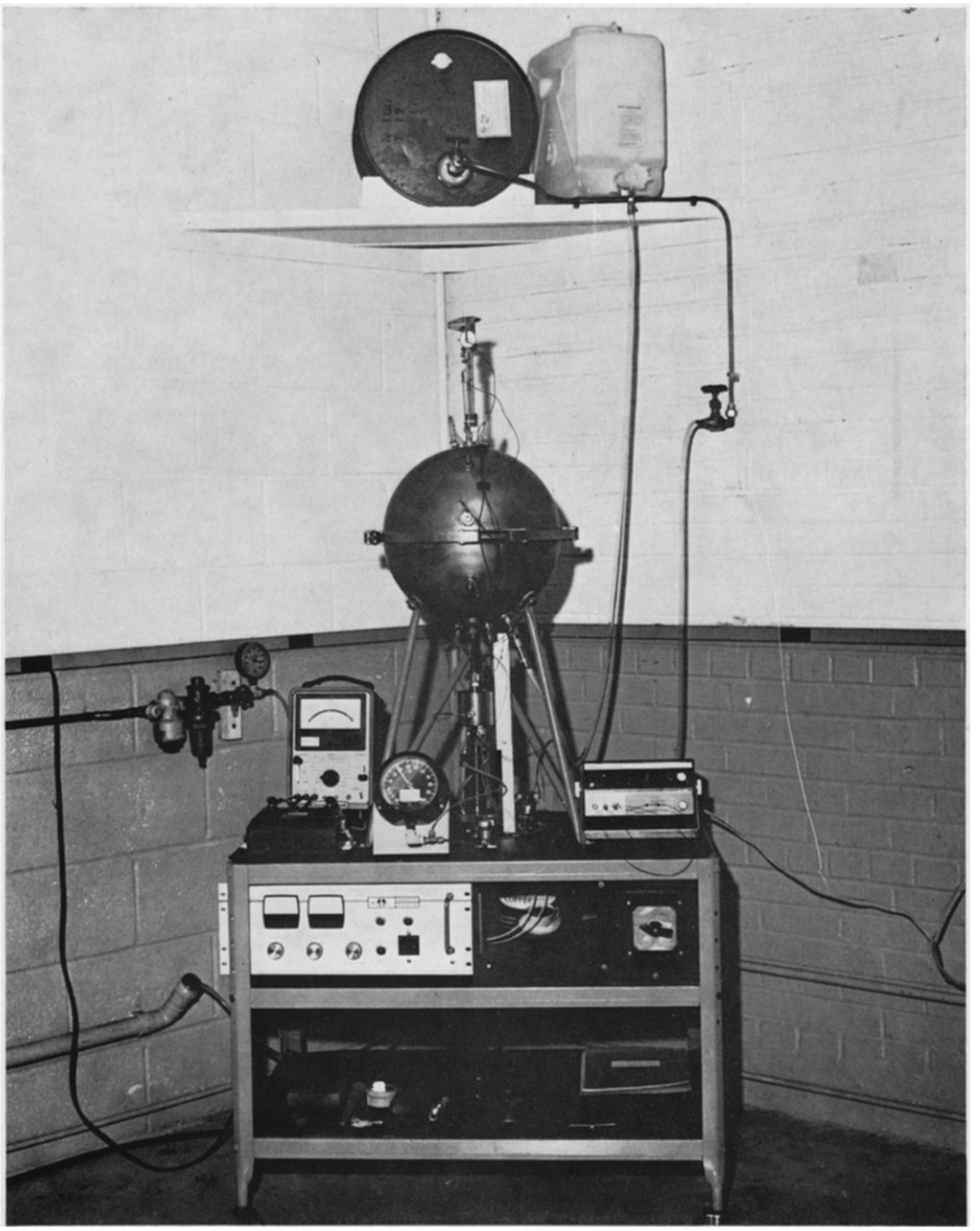

FIG. 1. Heat transfer apparatus.

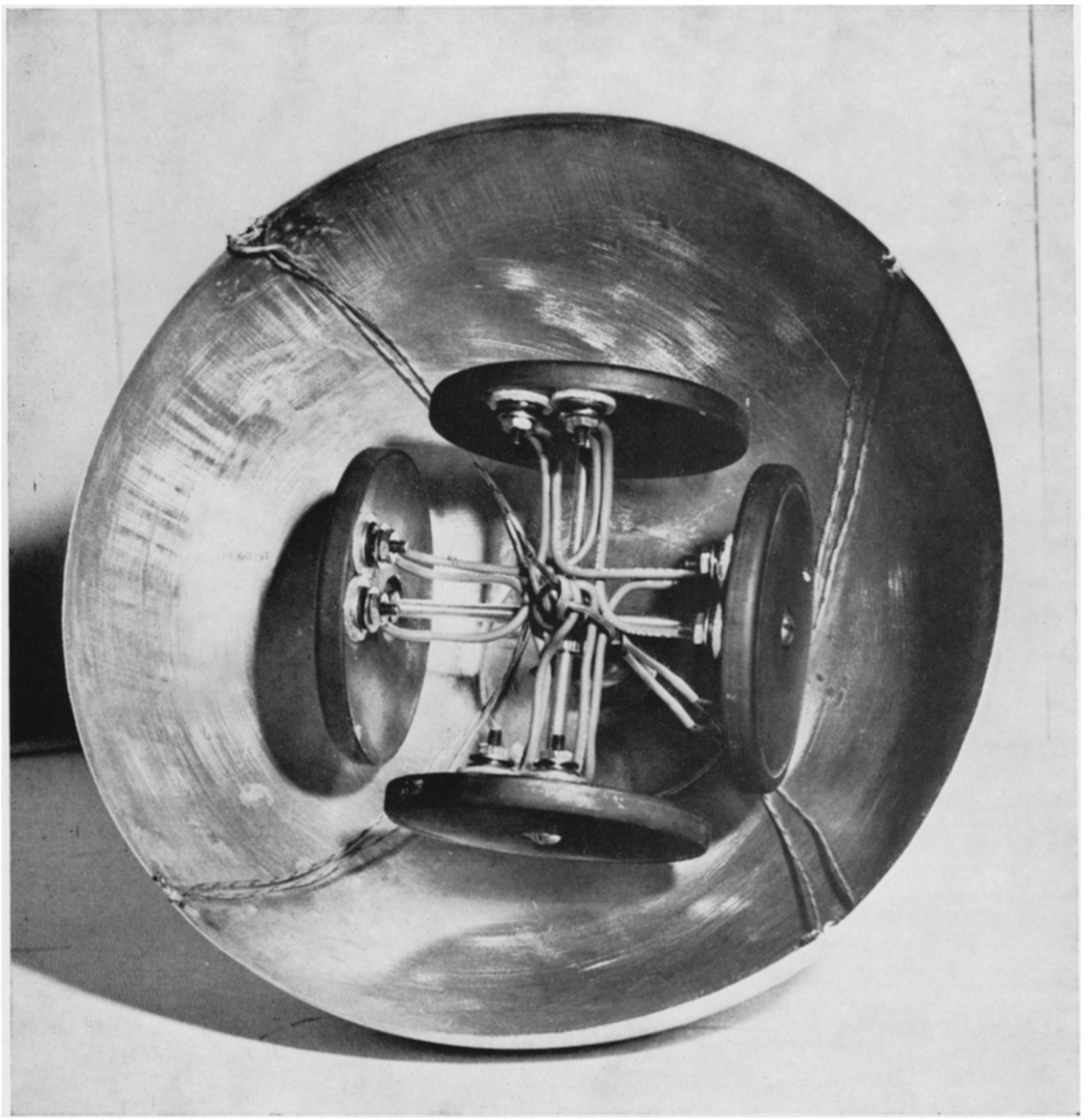

FIG. 2. Interior of inner sphere.

was attached by screws to permit removal of the sphere from the water jacket.

The water jacket was made of two, 35·6 cm dia., stainless steel hemispheres joined by an external gasketed flange to permit disassembly.

O-ring seals and was connected to a small cylindrical, stainless steel reservoir. The reservoir provided means of connecting electrical leads to the disk heaters, leads to the inner-sphere surface thermocouples, and the pressure probe to

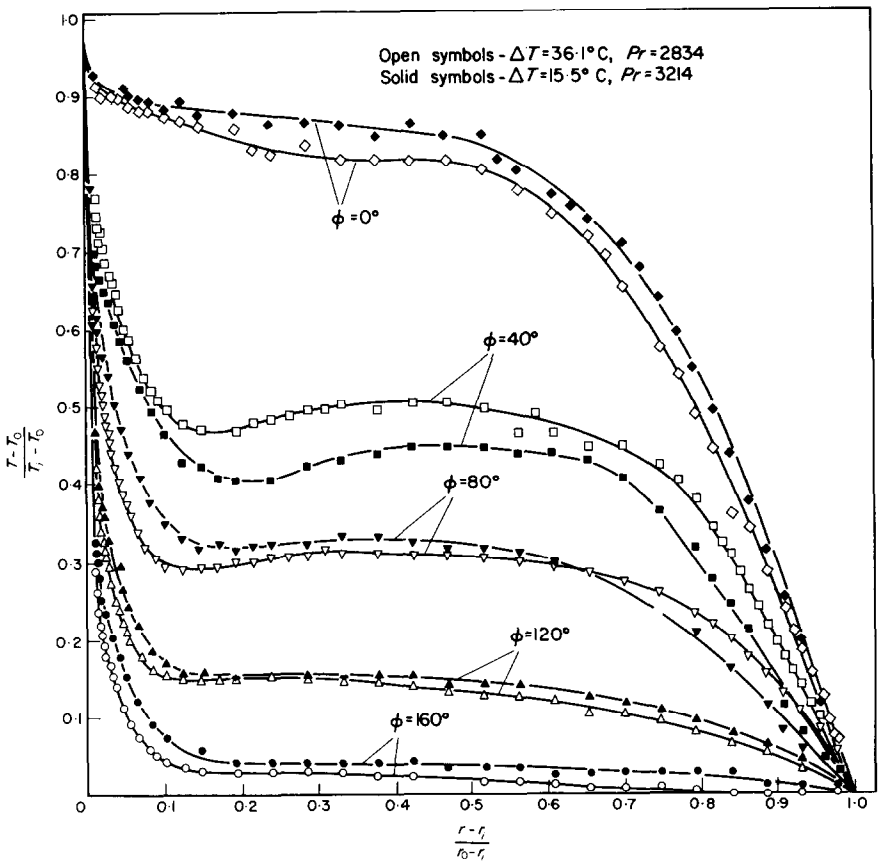

FIG. 3. Variation of temperature profiles with ΔT for 350 fluid, $L/r_i = 0{\cdot}79$.

The water, which maintained the outer sphere at a uniform temperature, was introduced at the base and withdrawn at the top through manifold systems. The outer-sphere surface temperature was taken to be the average of the inlet and outlet water temperatures, which were measured by thermocouples.

The inner-sphere support-stem passed through the outer-sphere and the water jacket through

instrumentation; it also provided means for charging the inner sphere with Freon-11. The reservoir rested on a threaded rod which was used to position the inner sphere along the vertical diameter within the outer sphere.

The thermocouple probes used to obtain the temperature profiles were constructed by inserting 24-gauge copper and constantan wires through 15-gauge stainless steel support tubes

and fusing the wires to form small junctions. The wires were then sealed to the tubes at both ends with epoxy cement. Each support tube was attached to a micrometer probing mechanism which could advance the thermocouple probe

200 Fluid-20 CS, and Dow-Corning 200 Fluid-350 CS in the gap. The Dow Corning 200 fluids are silicone base fluids, and the 20 CS and 350 CS designations refer to the kinematic viscosity in centistokes at 25°C. Henceforth, these fluids

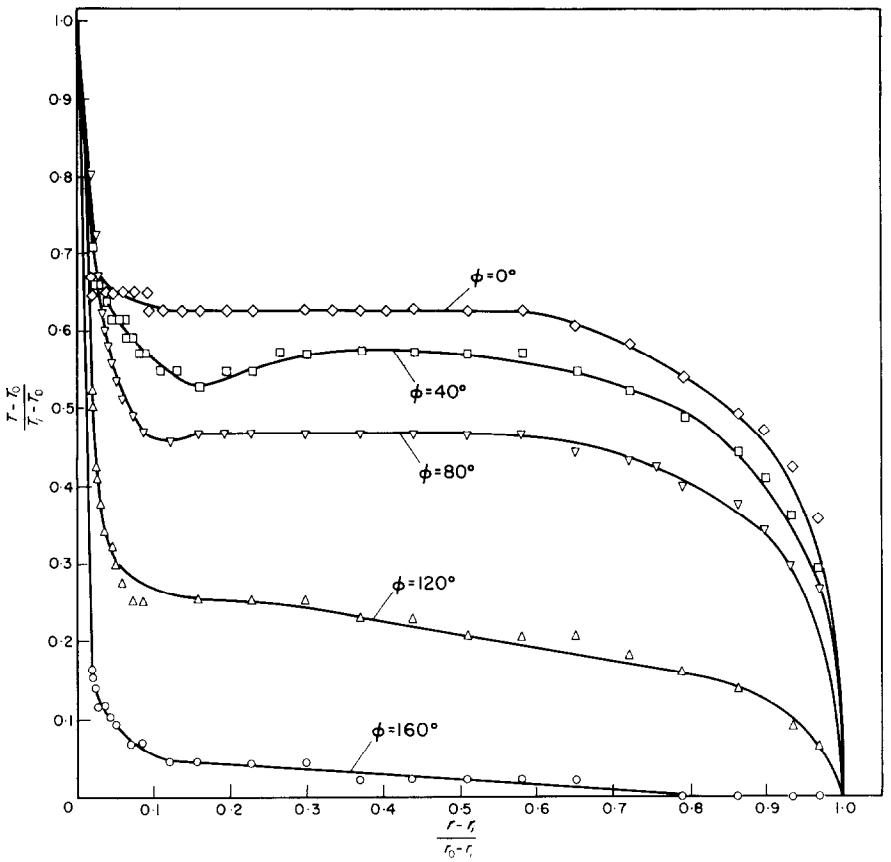

FIG. 4. Temperature profiles for water, $L/r_i = 0{\cdot}40$, $\Delta T = 10{\cdot}8°C$, $Pr = 6{\cdot}6$.

and indicate its position to within 0·003 cm. On the basis of previous work [1–3] the flow was assumed to be axisymmetric. Thus, five thermocouple probes were placed in a common vertical plane through the center of the spheres and were spaced at 40° intervals beginning with a probe on the upward vertical axis, $\phi = 0°$.

A total of approximately 470 heat-transfer runs were conducted with water, Dow Corning

will be referred to as 20 and 350 fluids. At each of the five gap–radius ratios for each of the fluids tested, 25 to 30 different values of temperature difference ΔT were established by controlling the electrical power input to the heaters. The natural convection heat transfer rate q is the difference between the power input to the electrical heaters and the heat losses due to the supporting stem. Since the stem was well

insulated on its lateral surface, convection from the stem was considered to be negligible, and the total stem loss was taken to be conduction down the stem. Calculations showed that the stem conduction was less than 3 per cent of the total power input for the largest ΔT achieved. Table 1 gives the ranges of the independent variables; Grashof number Gr, Rayleigh number Ra, Prandtl number Pr and gap–radius ratio L/r_i. The subscripts on Gr and Ra indicate the geometric dimension upon which these parameters are based. Sufficient time was allowed for establishment of a steady state before each run. At selected temperature differences (small, intermediate and large) for each gap–radius ratio and test fluid, temperature traverses were made utilizing the thermocouple probes.

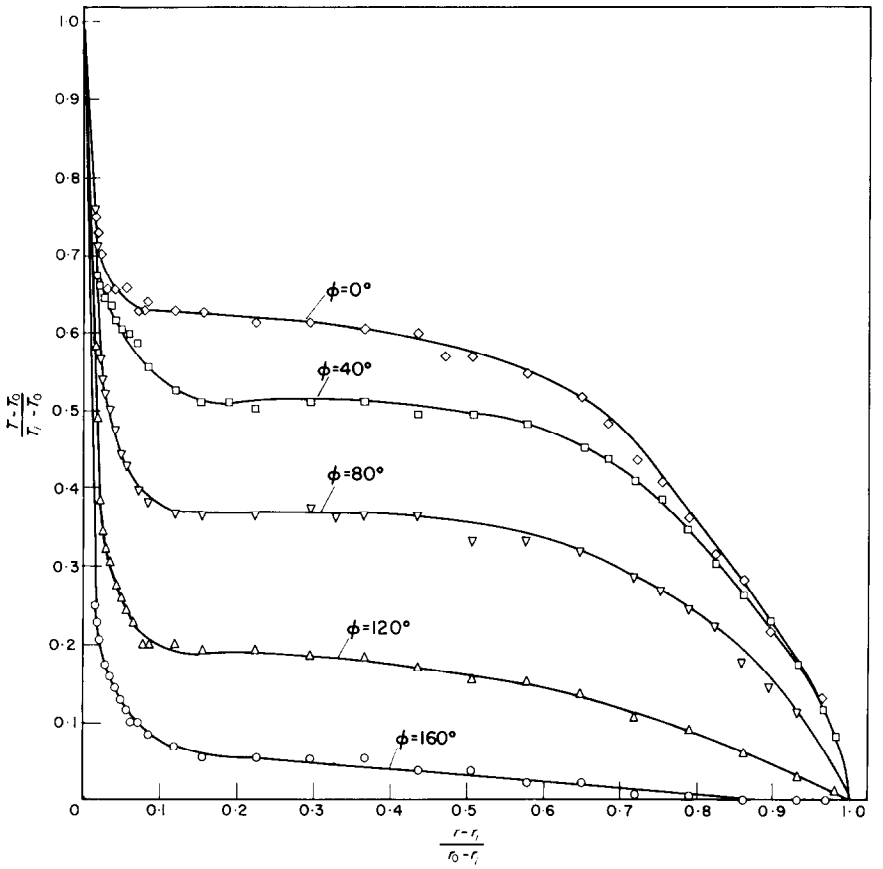

FIG. 5. Temperature profiles for 20 fluid, $L/r_i = 0{\cdot}40$, $\Delta T = 16{\cdot}3°C$, $Pr = 232$.

Table 1. Ranges of independent variables

Variable	Minimum value	Maximum value
Gr_L	$4{\cdot}0 \times 10^{-1}$	$1{\cdot}3 \times 10^{8}$
Ra_L	$1{\cdot}3 \times 10^{3}$	$5{\cdot}4 \times 10^{8}$
Pr	4·7	4148
L/r_i	0·09	1·81

3. TEMPERATURE DISTRIBUTION

Profiles of temperature T vs. radial position r were obtained at selected values of ΔT and angular positions ϕ for each value of L/r_i and test fluid. For each fluid investigated, the ΔT. Such fluctuations are interpreted as the result of unsteady flow, and meaningful profiles were not obtained under these conditions. Only those profiles for which there were no fluctuations are presented herein.

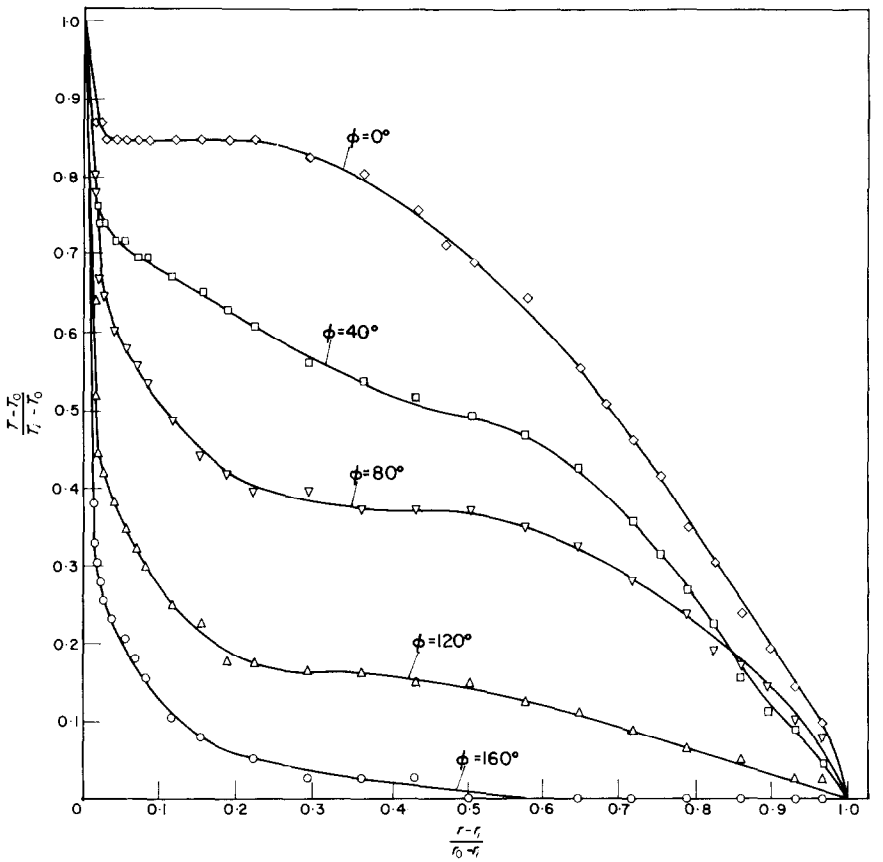

FIG. 6. Temperature profiles for 350 fluid, $L/r_i = 0{\cdot}40$, $\Delta T = 10{\cdot}8°C$, $Pr = 3422$.

behavior of the temperature profiles was found to follow consistent general trends for the four largest gap–radius ratios studied, and these will be discussed first. Next, the behavior of the profiles for the smallest gap–radius ratio, which did not follow the general trends, will be presented. It should be noted that temperature fluctuations of several degrees occurred for all values of L/r_i and test fluids at high values of

The form of the dimensionless temperature profile for a given value of ϕ was found to be independent of ΔT for a given L/r_i and test fluid when the Prandtl number remained essentially constant. Variations in the Prandtl number on the order of 15 per cent produce significant changes in the form of the temperature profile as ΔT varies; that is, the shape of the profile for a given angular position remains essentially the

same, but the magnitude of the temperature changes for a given radial position. Figure 3 shows the relative independence of the dimensionless temperature profiles on the temperature difference for an approximately 10 per cent

fluids are presented in Figs. 4–6 respectively. Since these profiles are for cases which satisfy the conditions required for the form of the profile to be independent of the temperatre difference, the same ΔT for each profile is not

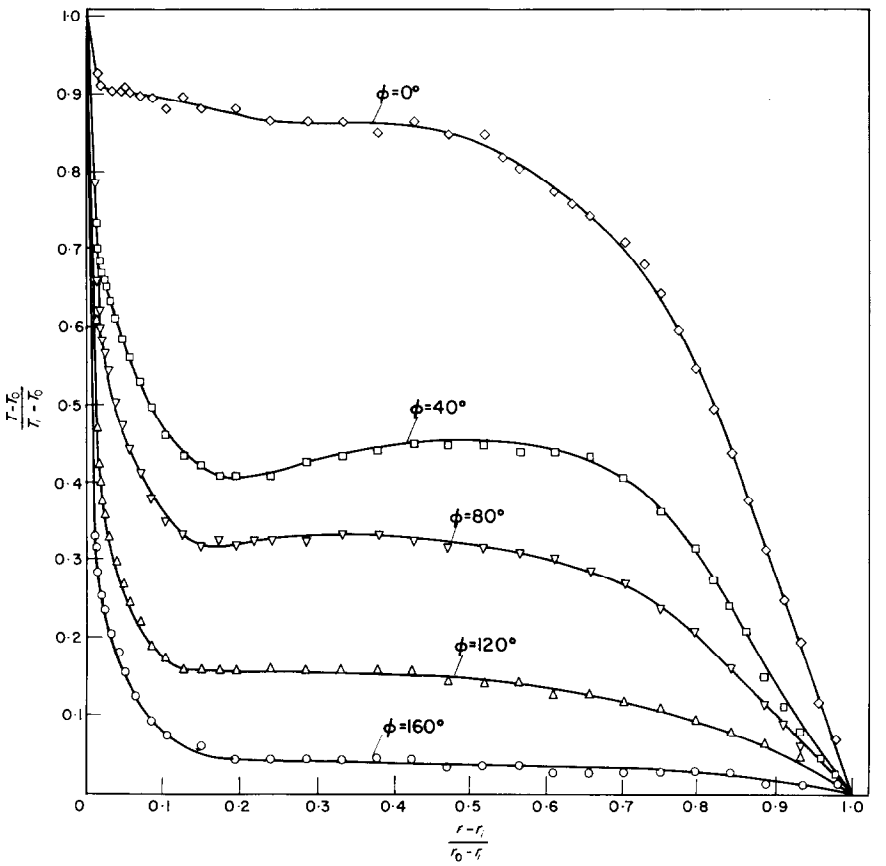

FIG. 7. Temperature profiles for 350 fluid showing temperature inversions, $L/r_i = 0{\cdot}79$, $\Delta T = 15{\cdot}5°C$, $Pr = 3214$.

variation in the Prandtl number for the 350 fluid and for a gap–radius ratio of 0·79. Since all the profiles presented are dimensionless, the adjective "dimensionless" will not be used in the discussion to follow.

For a given L/r_i, the manner in which the temperature profile varies from one fluid to another will now be considered. The temperature profiles for L/r_i of 0·40 for water, 20 and 350

necessary for the following comparison. The features of each profile shown in these figures are similar. Each profile may be conveniently described by five distinct regions which may vary, both in radial extent and in the magnitude of its characterizing feature, with angular position and the test fluid. These regions are defined in the same manner as in [1]; that is, a precipitous drop region immediately adjacent to the

inner-sphere surface, an inner-sphere curvature region, a region of small temperature gradients, an outer-sphere curvature region and a precipitous drop region immediately adjacent to the outer-sphere surface. Both the inner- and outer-sphere precipitous drop regions result from the high rate of heat convection through the thin high velocity boundary layers near the sphere surfaces. For all test fluids, as ϕ is increased from 0° the magnitude of the inner-sphere precipitous drop increases and that of the outer-sphere precipitous drop decreases. The magnitude of the inner-sphere precipitous drop is, in general, greater than that of the outer-sphere precipitous drop due to the larger velocity in the boundary layer adjacent to the inner sphere. Both inner- and outer-sphere curvature regions result from transition from high speed boundary layer flow to the low speed flow in the central portion of the gap. The region of small temperature gradients, except at $\phi = 0$, is a consequence of the low speed flow in this region. Note that the magnitude of the temperature within this region decreases with increasing ϕ. This is explained by the fact that the fluid is continuously heated by the inner sphere as ϕ decreases and cooled by the outer sphere as ϕ increases. The existence of a corner eddy at $\phi = 0$ causes the unique shape of the profile at this location, and the reader is referred to [1] for a detailed explanation of the phenomena involved.

The three fluids, (water, 20 and 350), gave Prandtl number ranges of 4·7–12, 148–336 and 1954–4148 respectively. As the Prandtl number is increased from one range to another (Figs. 4–6), the radial extent of both the inner-sphere and the outer-sphere curvature regions increases due to the thickening of the boundary layers. Figure 6 shows that for a Prandtl number of about 3420 the inner- and outer-sphere curvature regions extend throughout the gap for all angular positions except $\phi = 160°$. In the vicinity of $\phi = 160°$, where the hotter surface is primarily above the colder, it would be expected that conduction, rather than convection, would prevail. As shown in the photographs of flow patterns in [2], there is almost no convective activity in the region of 160° for the case of air, and it is expected that a similar situation should exist for the case of the fluids under discussion here. In fact, the similarity of these profiles with those for air indicates that this is so.

As L/r_i is changed, no exceptions to the general trends discussed above were noted, although the extents of the five regions and the magnitude of their characterizing features varied. Temperature inversions were observed in at least one angular position for all test fluids and values of L/r_i when Ra_L was greater than approximately 5×10^5. Figure 7 shows an example of such an inversion. These inversions are thought to be due to the high rate of angular convection of heat relative to radial transport of heat. Such inversions have also been observed in natural convection in cylindrical annuli by Liu *et al.* [5].

The temperature profiles obtained for the smallest value of L/r_i (0·09) for the three fluids tested do not follow the general trend. Figures 8–10 show the profiles for the three fluids in the order of increasing Prandtl numbers. From these figures it is noted that the magnitude of the temperature for a given position did not decrease consistently with increasing values of ϕ, and the extent of the curvature regions is considerably less than for the cases of large L/r_i. Figure 8 shows that for water, within experimental accuracy, the temperature at every radial position within the gap was greatest for $\phi = 40°$, next greatest for $\phi = 80°$, followed by 0, 120 and 160° in that order. This ordering of the magnitudes of T for $\phi = 0$ and 40°, relative both to each other and to those for the other angular positions, is almost totally different from that of any other gap–radius ratio; however, the ordering of the magnitudes of T for $\phi = 80$, 120 and 160° relative to each other does follow the general rule. This ordering of the temperature profiles can be explained by the postulation of a multicellular flow pattern consisting of a large cell extending from the lower vertical axis up through and including $\phi = 40°$ and an arbitrary

odd number of cells between $\phi = 0°$ and $\phi \cong 40°$. An unusual ordering of the profiles for small values of L/r_i was also found for air as reported in [1]. It is observed from Figs. 8–10 that as Prandtl number is increased the same relative order of the profiles for $\phi = 80$, 120 and considering the large cell to now extend only up to and including $\phi = 80°$.

4. HEAT-TRANSFER RESULTS

The heat transfer results which were obtained experimentally are analyzed in terms of the

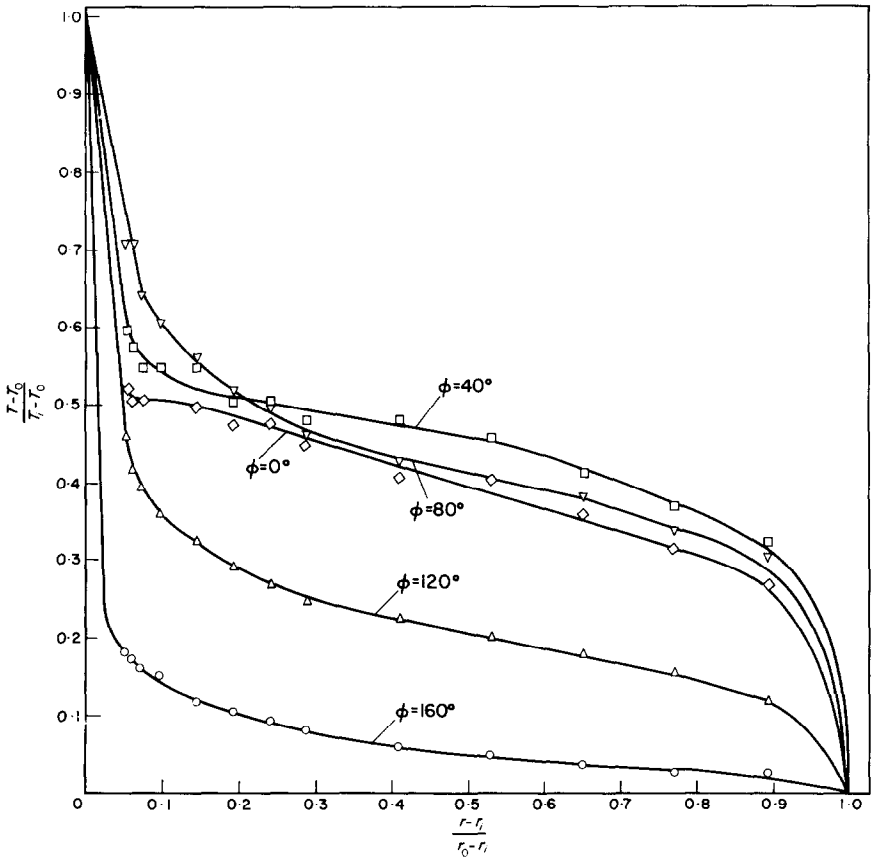

FIG. 8. Temperature profiles for water, $L/r_i = 0{\cdot}09$, $\Delta T = 11{\cdot}1°C$, $Pr = 7.6$.

160° is maintained, although the 0 and 40° profiles are shifted. The profile for $\phi = 40°$ falls below that for $\phi = 80°$ for both cases of Prandtl number higher than that of water. This indicates a decrease in the size of the large cell as Prandtl number increases. The ordering of the temperature profiles for the higher Prandtl numbers shown in Figs. 9 and 10 can be explained by following independent parameters: Rayleigh number or Grashof number, Prandtl number and the gap–radius ratio. The heat transfer results for air which are presented in [1] will be treated along with the present data. In that work with air it was found that the results were best correlated by using an effective thermal conductivity ratio k_{eff}/k defined in the following

manner

$$k_{eff}/k = \frac{qL}{4\pi k(\Delta T) r_i r_0}. \quad (1)$$

This definition will also be used herein. The foregoing dimensionless parameters were calculated using properties evaluated at a volume-weighted mean temperature which is defined by

$$T_m = [(r_{av}^3 - r_i^3)\, T_i + (r_0^3 - r_{av}^3) T_0]/(r_0^3 - r_i^3). \quad (2)$$

It was anticipated that the heat transfer results could be correlated by a functional relationship of the form

$$k_{eff}/k = f(Ra, Pr, L/r_i) \quad (3)$$

or

$$k_{eff}/k = f(Gr, Pr, L/r_i). \quad (4)$$

Before any attempt was made to obtain an overall correlation equation for all of the experimental results, a specific correlation equation was first sought for the case of each fluid. In analyzing the experimental data it was observed that plots of k_{eff}/k vs. Ra or Gr for each L/r_i resulted in straight lines on log–log coordinates. This suggested that equations of the type

$$k_{eff}/k = CRa^a\, Pr^b\, (L/r_i)^c \quad (5)$$

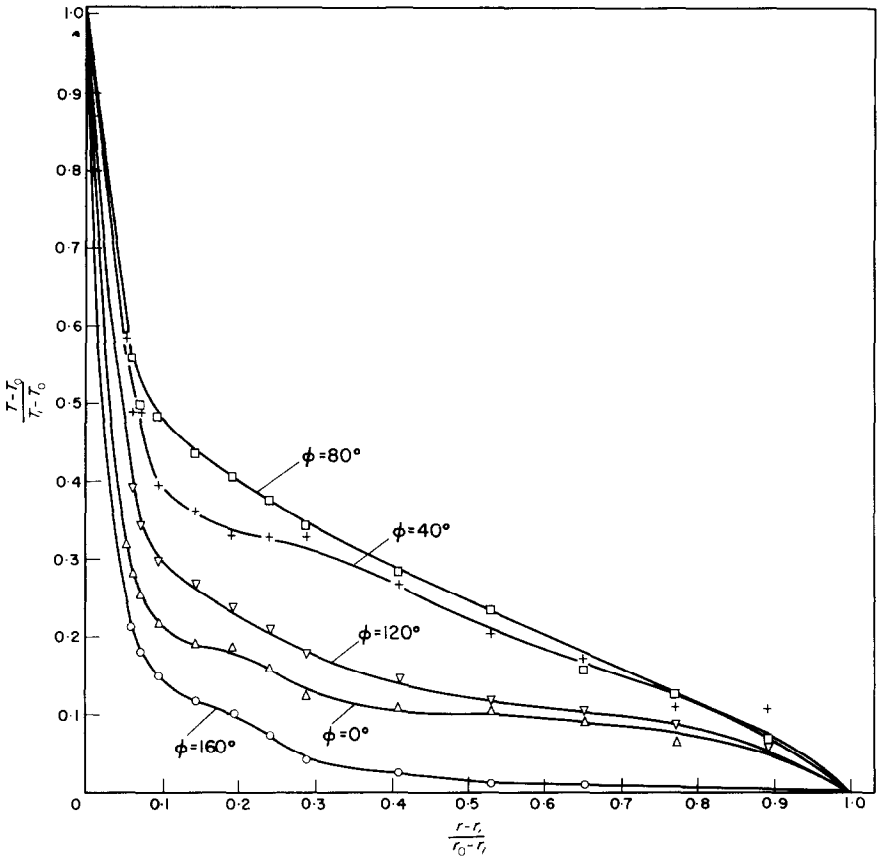

FIG. 9. Temperature profiles for 20 fluid, $L/r_i = 0{\cdot}09$, $\Delta T = 8°C$, $Pr = 269$.

or

$$k_{\text{eff}}/k = CGr^a Pr^b (L/r_i)^c \quad (6)$$

might prove suitable. In these expressions Ra and Gr were based on L, r_i or r_0 and r_0/r_i was used in addition to L/r_i; also a conventional Nusselt number was used in addition to k_{eff}/k. An equation of the form developed by Eckert and Drake [6] and utilized by Liu *et al.* [5] for correlating results for cylindrical annuli to account for Prandtl number variations was also used. In addition, fluid properties were evaluated at arithmetic mean temperatures as well as at T_m.

Considering the data for each fluid individually, good results were obtained by an equation of the form

$$k_{\text{eff}}/k = CRa_L^a \quad (7)$$

where fluid properties were evaluated at T_m. The empirical constants in this equation are tabulated in Table 2 and the resulting equations are shown plotted along with the experimental data in Fig. 11.

Slightly greater apparent accuracy was obtained using equations of the form

$$k_{\text{eff}}/k = CRa_L^a (L/r_i)^b \quad (8)$$

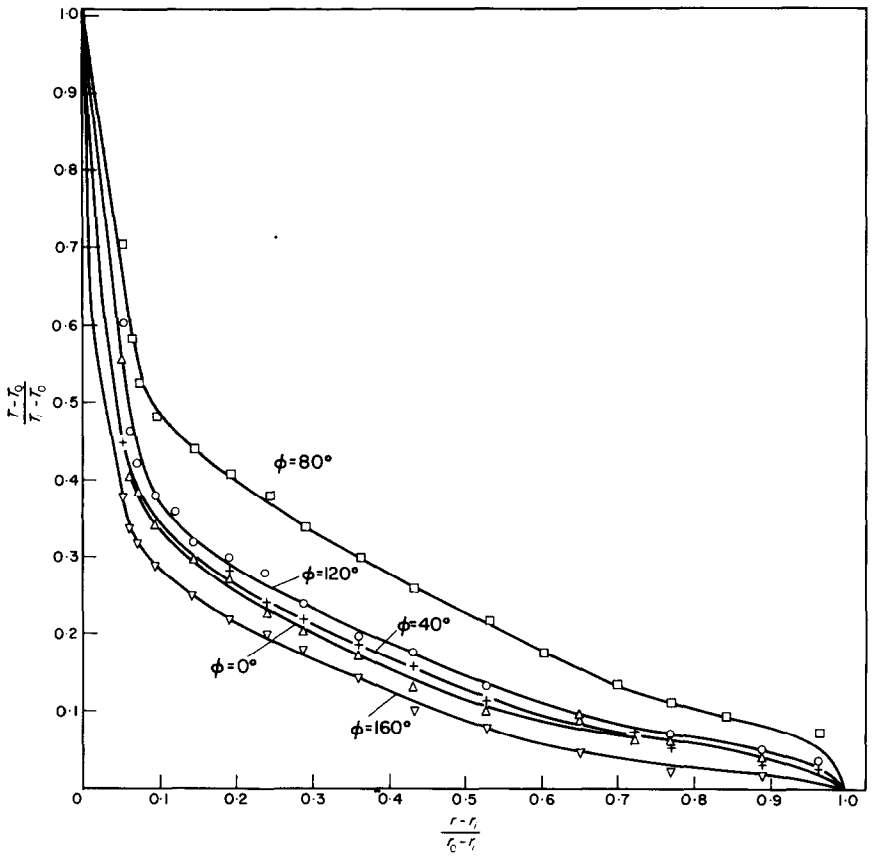

FIG. 10. Temperature profiles for 350 fluid, $L/r_i = 0{\cdot}09$, $\Delta T = 12{\cdot}0°C$, $Pr = 3302$.

but the apparent improvement due to the additional empirical constant is not justified. For comparison purposes the results obtained utilizing equation (8) are shown in Table 3.

It is evident from Fig. 11 that a single equation of the form of equation (7) will not satisfactorily correlate the data for all of the test fluids. In the search for a correlation equation for all of the test fluids, all equation forms used for each individual fluid were evaluated. It was found that

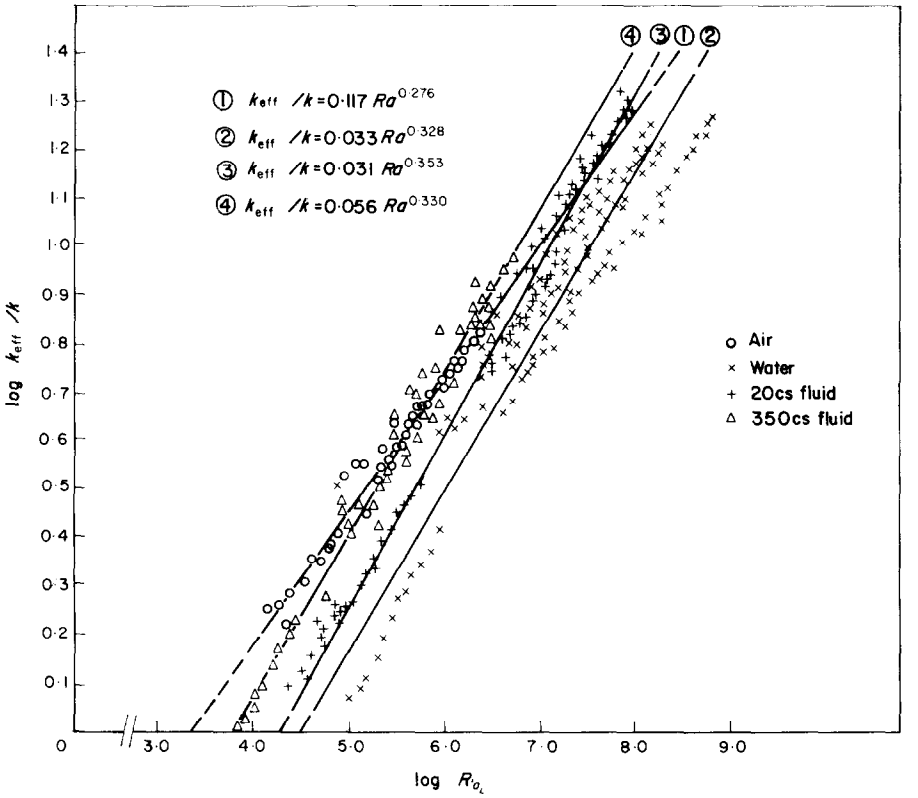

FIG. 11. Heat-transfer correlations for individual fluids.

Table 2. Empirical constants and deviations for equation (7)

Fluid	C	a	Average per cent deviation	Per cent of data within ±20 per cent of equation
air	0·117	0·276	4·0	98·6
water	0·033	0·328	15·7	71·4
20 CS	0·031	0·353	7·1	98·6
350 CS	0·056	0·330	6·5	96·6

Table 3. Empirical constants and deviations for equation (8)

Fluid	C	a	b	Average per cent deviation	Per cent of data within ±20 per cent of equation
air	0·162	0·252	0·059	3·9	98·6
water	0·078	0·279	0·155	13·4	79·6
20 CS	0·072	0·305	0·124	6·0	97·9
350 CS	0·104	0·288	0·110	5·3	97·5

the best correlation was given by

$$k_{\text{eff}}/k = 0{\cdot}202\, Ra_L^{0{\cdot}228}\,(L/r_i)^{0{\cdot}252} Pr^{0{\cdot}029} \quad (9)$$

with an average deviation of 13·7 per cent. (The deviation at a particular data point is defined as the absolute difference between the data and the equation value divided by the data value; the average per cent deviation is the sum of these individual deviations divided by the total number of data points.) Since the exponent of Ra_L is nearly equal to the exponent of L/r_i and since the exponent of Pr is so small, L/r_i and Ra_L were combined into one parameter defined as Ra^*, and Pr was eliminated. The resulting equation

$$k_{\text{eff}}/k = 0{\cdot}228\,(Ra^*)^{0{\cdot}226} \quad (10)$$

gives an average deviation of 15·6 per cent, and 76 per cent of the data are within ±20 per cent of values predicted by the equation. Even though equation (10) is slightly less accurate than equation (9), its use is recommended over that of equation (9) since it contains only two empirical constants rather than four. Equation (10) is shown plotted along with the experimental data in Fig. 12. It is evident from this figure that the largest amount of scatter from equation (10) occurs with the data obtained

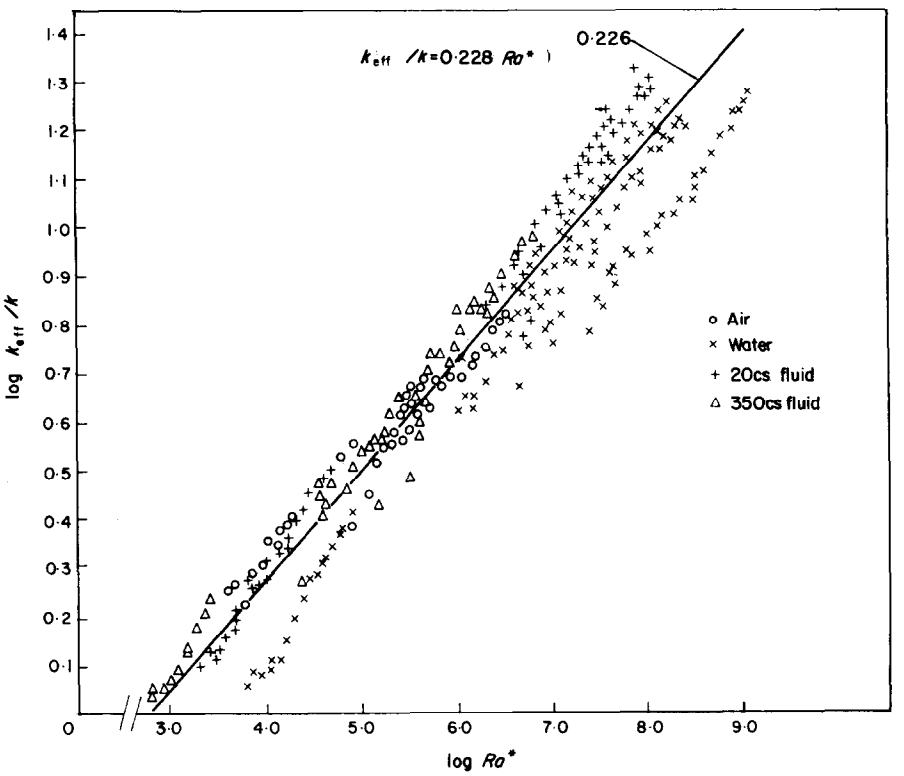

FIG. 12. Overall heat-transfer correlation.

using water. It is interesting to note that the Pr effect and the L/r_i effect can be taken into account by use of Ra^* without significant loss of accuracy.

To summarize the above, it is recommended that the following equations be used within the indicated Ra and Pr ranges

$$1{\cdot}4 \times 10^4 < Ra_L < 2{\cdot}5 \times 10^6, \quad Pr = 0{\cdot}7: \quad k_{\text{eff}}/k = 0{\cdot}117\, Ra_L^{0{\cdot}276} \tag{11a}$$

$$2{\cdot}4 \times 10^4 < Ra_L < 5{\cdot}4 \times 10^8, \quad 4{\cdot}7 < Pr < 12{\cdot}1: k_{\text{eff}}/k = 0{\cdot}033\, Ra_L^{0{\cdot}328} \tag{11b}$$

$$2{\cdot}4 \times 10^4 < Ra_L < 9{\cdot}7 \times 10^7, \quad 148 < Pr < 336: k_{\text{eff}}/k = 0{\cdot}031\, Ra_L^{0{\cdot}353} \tag{11c}$$

$$1{\cdot}3 \times 10^3 < Ra_L < 5{\cdot}6 \times 10^6, \quad 1954 < Pr < 4148: k_{\text{eff}}/k = 0{\cdot}056\, Ra_L^{0{\cdot}330} \tag{11d}$$

$$1{\cdot}2 \times 10^2 < Ra^* < 1{\cdot}1 \times 10^9, \quad 0{\cdot}7 < Pr < 4148: k_{\text{eff}}/k = 0{\cdot}228\,(Ra^*)^{0{\cdot}226}. \tag{11e}$$

All of the foregoing equations are restricted to $0{\cdot}09 < L/r_i < 1{\cdot}81$ and fluid properties evaluated at T_m. Use of the overall equation is recommended in cases where the first four equations are not specifically applicable.

5. CONCLUSION

This paper reports the results of a study of natural convection between isothermal concentric spheres. Both temperature profiles and heat-transfer rates are reported for a wide range of gap–radius ratios, Rayleigh numbers and Prandtl numbers.

The experimentally determined temperature profiles were found to be relatively independent of the temperature difference between the two spheres for all but the smallest gap–radius ratio considered and for variations in the Prandtl number less than about 15 per cent. Larger Prandtl number variations produced significant changes in the magnitude of the temperature at a given point in the gap, although the shape of the profiles remained essentially the same. It was found that the temperature distributions for all the gap–radius ratios considered could be described in terms of five distinct regions, as previously defined in reference [1]. For the four largest values of L/r_i considered, the changes in the temperature profiles with Prandtl number were explained in terms of boundary layer phenomena, and no significant changes in the general trends were observed as L/r_i was varied. Temperature inversions, believed to be caused by a high rate of angular convection of heat relative to the radial transport, were observed for a variety of test conditions.

The behavior of the temperature profiles for the smallest value of L/r_i, 0·09, was explained by postulating the existence of a large cell extending from the lower vertical axis into the upper portion of the gap and an arbitrary odd number of smaller cells occupying the remainder of the gap. This large cell apparently decreases in size as the Prandtl number increases. The postulation of multicellular flow is consistent with previously observed results for air with small values of L/r_i [1].

It was found that the heat-transfer results, both for each fluid individually and for all the data combined, could be correlated simply in terms of k_{eff}/k and a Rayleigh number. For each individual fluid Ra_L was utilized, while for all the data combined Ra^* was used. These relationships are given by equations (11). Use of the equations having the more restricted Prandtl number ranges is recommended whenever possible since they are slightly more accurate than the overall equation. However, all of these equations reproduce the experimental data to within an average deviation of less than 16 per cent. It is significant to note that an overall heat-transfer correlation which does not involve explicit use of Pr and L/r_i was obtained even though large variations in these parameters were considered in the investigation.

It is believed that the results described herein represent the only information currently available concerning natural convection heat transfer between concentric spheres at a Prandtl number other than about 0·7. The work reported herein

concentrated on obtaining heat transfer and temperature profile results. Future work should be directed toward a determination of more detailed effects, such as the specific flow patterns which occur for wide variations in the Rayleigh number, Prandtl number and gap radius ratio.

ACKNOWLEDGEMENTS

The work reported on in this paper was supported by the Atomic Energy Commission under contract AT (45-1)-2214 and by the Endowment and Research Foundation of Montana State University.

REFERENCES

1. E. H. BISHOP, L. R. MACK and J. A. SCANLAN, Heat transfer by natural convection between concentric spheres, *Int. J. Heat Mass Transfer* **9**, 649–662 (1966).
2. E. H. BISHOP, R. S. KOLFLAT, L. R. MACK and J. A. SCANLAN, Convective heat transfer between concentric spheres, *Proc.* 1964 *Heat Transfer and Fluid Mechanics Institute*. Stanford University Press, pp. 69–80 (1964).
3. E. H. BISHOP, R. S. KOLFLAT, L. R. MACK and J. A. SCANLAN, Photographic studies of convection patterns between concentric spheres, *Soc. Photo-Optical Instrumentation Engrs Jl* **3**, 47–49 (1964–1965).
4. L. R. MACK and H. C. HARDEE, Natural convection between concentric spheres at low Rayleigh numbers, *Int. J. Heat Mass Transfer* **11**, 387–396 (1968).
5. C. Y. LIU, W. K. MUELLER and F. LANDIS, Natural convection heat transfer in long horizontal cylindrical annuli, *International Developments in Heat Transfer*, paper 117, Part V, ASME, pp. 976–984 (1961).
6. E. R. G. ECKERT and R. M. DRAKE, *Heat and Mass Transfer*, pp. 313–315. McGraw-Hill, New York (1959).

CONVECTION THERMIQUE NATURELLE ENTRE DEUX SPHÈRES CONCENTRIQUES

Résumé—On considère dans une étude expérimentale la convection naturelle entre deux sphères concentriques isothermes dont le rapport des diamètres varie entre 1,09 et 2,8. Les fluides convectant utilisés sont l'eau et deux huiles silicones correspondant à des nombres de Prandtl compris entre 4,7 et 4,148 et des nombres de Rayleigh, basés sur la valeur de l'écartement variant de $1{,}3 \cdot 10^3$ à $5{,}8 \cdot 10^8$. Les profils de température mesurée sont analysés en détail par référence aux cinq formes de profil caractéristiques. Toutes les allures de profil sont expliquées à partir de modèles d'écoulement convectif qui représentent les extensions du travail déjà publié pour l'air sous des conditions comparables. On représente pour chacun des trois fluides la variation de K_{eff}/K en fonction du nombre de Rayleigh et on présente une expression globale basée uniquement sur le nombre de Rayleigh modifié que unifie les résultats obtenus sur les trois liquides aussi bien que pour l'air.

Les corrélations représentent les résultats avec un écart moyen inférieur à 16 pour cent.

WÄRMEÜBERTRAGUNG DURCH NATÜRLICHE KONVEKTION ZWISCHEN KONZENTRISCHEN KUGELN

Zusammenfassung—Es werden experimentelle Untersuchungen beschrieben über natürliche Konvektion zwischen zwei konzentrischen isothermen Kugeln mit verschiedenen Durchmesserverhältnissen im Bereich von 1,09 bis 2,81. Als Versuchsflüssigkeiten wurden Wasser und zwei Silikonöle verwendet, die Prandtlzahlen im Bereich von 4,7 bis 4148 und Rayleighzahlen, gebildet mit der Spaltweite, im Bereich von $1{,}3 \cdot 10^3$ bis $5{,}8 \cdot 10^8$ lieferten. Die gemessenen Temperaturprofile werden genau ausgewertet in bezug auf fünf charakteristische Merkmale der Profilformen. Alle Profileigenheiten werden erklärt mit Hilfe postulierter Strömungsmuster, welche die Erweiterung einer Arbeit darstellen, die kürzlich unter ähnlichen Bedingungen für Luft durchgeführt wurde. Für jede der drei Flüssigkeiten wird eine Beziehung für den Wärmeübergang aufgestellt zwischen k_{eff}/k und der Rayleighzahl. Ausserdem wird ein allgemeingültiger Ausdruck formuliert, der nur von einer modifizierten Rayleighzahl ausgeht und für alle drei Flüssigkeiten sowie für Luft gültig ist. Die Beziehungen stimmen mit den Messdaten bis auf eine durchschnittliche Abweichung von weniger als 16 Prozent überein.

ТЕПЛООБМЕН КОНЦЕНТРИЧЕСКИХ ШАРОВ ПРИ СВОБОДНОЙ КОНВЕКЦИИ

Аннотация—Описано экспериментальное исследование естественной конвекции между изотермическими концентрическими шарами из керамики при соотношениях диаметров от 1,09 до 2,81. В качестве рабочей среды использовались вода и два кремниевых масла при числах Прандтля от 4,7 до 4148 и числах Релея, отнесенных к ширине зазора в

диапазоне от $1{,}3 \times 10^3$ до $5{,}8 \times 10^8$. Подробно анализируются измеренные температурные профили для пяти типичных характеристик профиля шаров. Все свойства профилей объясняются с помощью постулированных конвективных режимов течения, что является обобщением опубликованной ранее работы для воздуха при аналогичных условиях. Получена корреляция в виде отношения между Ak_{eff}/k и числом Релея отдельно для каждой из трех жидкостей. Представлено также общее выражение, основанное только на модифицированном числе Релея, применимое для обобщения всех трех жидкостей, а также для воздуха. Это обобщение дает среднее отклонение меньше 16%.